05,13

Spatial division of spin wave signal in a waveguide based on a ferrimagnet/antiferromagnet structure

© A.S. Ptashenko[1], S.A. Odintsov[1], E.I. Salomatova[1], A.A. Amirov[2], A.V. Sadovnikov[1]

[1] Saratov National Research State University,
Saratov, Russia
[2] Amirkhanov Institute of Physics, Dagestan Federal Research Center, Russian Academy of Sciences,
Makhachkala, Russia

E-mail: andrey.po3@mail.ru

Received July 25, 2023
Revised July 25, 2023
Accepted August 1, 2023

A study on the propagation of spin waves in a waveguide based on a ferrimagnetic film of iron-yttrium garnet (YIG) with a longitudinally oriented layer of antiferromagnetic iron-rhodium (FeRh) has been conducted. The case where the transverse dimension of the FeRh layer is an order of magnitude smaller than the waveguide width is considered. By means of micromagnetic modeling, the problem of exciting surface spin waves in the antenna region and detecting the integral magnitude of the dynamic magnetization in the output section of the structure has been solved. It is shown that changing the temperature of the FeRh layer leads to a variation in the amplitude-frequency characteristics. Moreover, in the output section, there is a localization of the spin wave intensity either in the YIG region, underneath the FeRh layer, or in the free area of the film. This is caused by power division of the input signal due to the change in the magnetization of the FeRh layer. The proposed structure based on YIG/FeRh can be used as logical devices in magnonics and for spatial-frequency signal selection in magnonic networks.

Keywords: spin waves, magnonics, ferrimagnet/antiferromagnet, iron-yttrium garnet, iron-rhodium.

DOI: 10.61011/PSS.2023.10.57219.163

1. Introduction

Recently, magnetic materials with a first-order magnetic phase transition (FOMPT) are actively studied due to their potential applications in various fields, such as energy-efficient technologies, temperature monitoring systems, and memory devices [1,2]. The particular interest belongs to the intermetallic iron-rhodium (IR) alloy [3], which has a gigantic magnetocaloric effect [4] and colossal magnetoresistance at elevated temperatures [5].

Such alloys, close to equiatomic ratios, have an ordered crystal structure of the CsCl type. This means that their magnetization [6], lattice constants [7] and heat capacity [8] change in the temperature range 310−360 K. The study of methods and mechanisms to control the properties of spin waves in composite materials based on structures with FOMPT and media, in which spin waves (SW) propagate, is an urgent task. To vary the magnetic parameters of the IR layer, various approaches can be used, such as the influence of a magnetic field [9], hydrostatic pressure [10], electric field induced by deformation [11,12] and other methods. Magnonic waveguides can play a special role in gaining control over the dynamics of spin waves. They are structures consisting of a magnetic film in the form of a layer whose longitudinal dimension exceeds the transverse one, and are used to transmit signals between information processing devices [13,14]. The yttrium-iron garnet (YIG) is considered one of the materials most commonly used in studying the SW propagation due to YIG unprecedented low loss parameters and narrow ferromagnetic resonance linewidth. In this case, SW properties in YIG microwaveguides can be controlled by creating lamellar structures, such as, for example, YIG/piezoelectric [15], YIG/piezoelectric [16]. Using a combination of structures based on ferrimagnetic films and antiferromagnetic layers, more precise control of the characteristics of spin waves is possible [17–20].

In this paper we study the possibility to control the spin waves that propagate as guided modes of the combined YIG/IR structure. In this case, a layer of the IR alloy is placed on the YIG layer and leads to a transformation of the value of the internal magnetic field in the area of YIG microwaveguide. Using micromagnetic numerical simulation, the spectra of the spin waves transmission through a composite double-layer microwaveguide were obtained. Analysis of the obtained results showed that the proposed structure can be used as a functional block in planar magnonic networks, for example, as a mode filter. Moreover, the possibility to control the spin wave signals propagation by changing the temperature of the IR layer was demonstrated. These results confirm the perspectives of this combined structure in the development of new magnetic materials and devices based on them, which is currently relevant for the development of computing approach based on magnonic logic [21].

2. Structure under study

Let us consider a structure consisting of YIG microwaveguide ($Y_3Fe_5O_{12}$) and a IR layer. The YIG microwaveguide

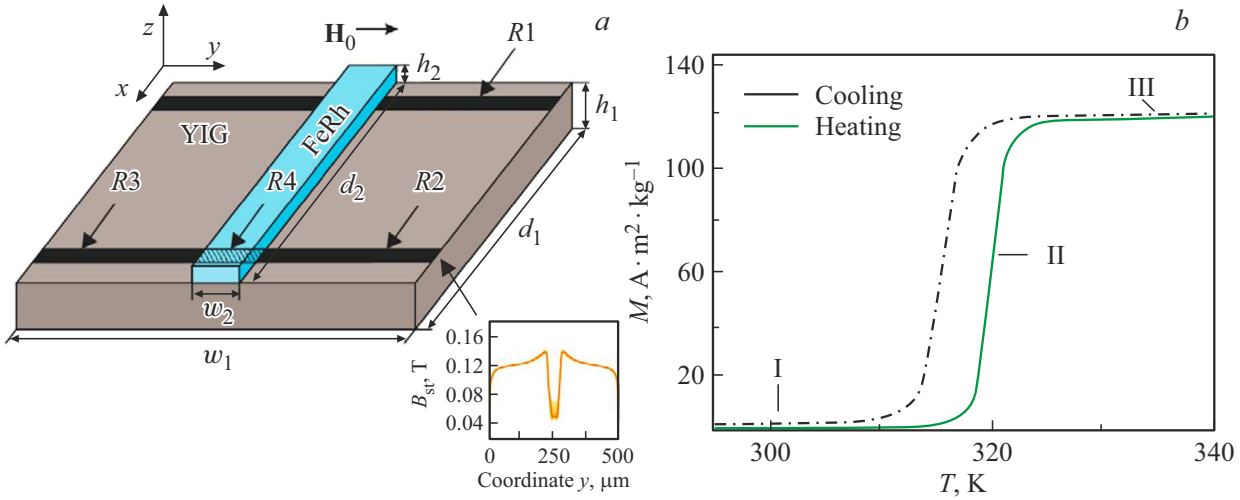

Figure 1. *a* — diagram of the YIG microwaveguide under consideration with IR layer located on it; *b* — experimentally obtained temperature dependence of the magnetization of the alloy $Fe_{48}Rh_{52}$ (green — heating, black — cooling).

is traditionally grown on a gallium gadolinium garnet (GGG) substrate. YIG has a saturation magnetization $M_S = 139$ kA/m and a ferromagnetic resonance linewidth $\Delta H = 0.54$ Oe. The dimensions of the YIG/IR microwaveguide are shown in Figure 1, *a* and are: length $d_1 = 7000\,\mu$m, width$w_1 = 500\,\mu$m, and thickness $h_1 = 10\,\mu$m. The LR layer is located in the center of the structure above the YIG film and has the following dimensions: length $d_2 = 7000\,\mu$m, width $w_2 = 50\,\mu$m, height $h_2 = 30\,\mu$m.

Segment R1 in Figure 1, *a* denotes the region of SW excitation located across the entire microwaveguide, and regions R2, R3 and R4 are the signal detection regions in YIG outside and under the IR layer, respectively. The structure is placed in the external static magnetic field $H_0 = 1200$ Oe, oriented along the axis y to effectively excite a surface magnetostatic wave (SMW) [22,23]. IR alloys with composition close to equiatomic and ordered in a CsCl-type structure are characterized by an isostructural metamagnetic transition from the antiferromagnetic (AFM) phase to the ferromagnetic (FM) phase at temperatures close to room temperature. This leads to a sharp change in magnetization [13]. For this study, the characteristics of the alloy $Fe_{48}Rh_{52}$ [13] were used. The experimentally obtained in paperwork [13] temperature dependence of magnetization is shown in Figure 1, *b*.

For numerical modeling three characteristic points were selected, indicated in Figure 1, *b*, and corresponding to three levels of temperature/magnetization in the IR alloy: $M_{sat} = 0$ kA/m, $M_{sat} = 40$ kA/m, $M_{sat} = 120$ kA/m. Next, we will consider how the modes of SW propagation change in the combined YIG/IR structure at different values of temperature and magnetization of IR.

3. Numerical modelling method

To study the spin waves propagation in the structure the micromagnetic modeling (MM) was used applying MuMax3 program [24]. This modeling uses a numerical solution to the Landau–Lifshitz–Gilbert equation, which describes the precession of the magnetic moment M in the effective magnetic field $H_{eff} = H_0 + H_{demag} + H_{ex} + H_a$, consisting of an external magnetic field H_0, demagnetization field H_{demag}, exchange field H_{ex} and anisotropy field H_a. In this study we assumed the anisotropy field to be equal to zero ($H_a = 0$), since YIG equilibrium magnetization vector is directed along the symmetry axes of the crystal.

To reduce signal reflections from the boundaries of the computational domain during numerical simulation, regions with increased attenuation coefficient $\alpha = 10^{-5}$ were introduced in the initial part of the input and the final part of the output section of the waveguide structure. This makes it possible to more accurately model the spin waves propagation without distortions caused by reflections from boundaries.

Using MM, we calculated the amplitude-frequency curves (AFC) of SW for the structure under study with different magnetization values of IR layer (Figure 2). Based on the analysis of the shown AFC plotted for the integral signal for m_z-component of the dynamic magnetization $\int_0^{y_{max}} m_z(x = x_s, y)dy$, obtained from antennas R2, R3 and R4 located in the section $x = x_s$, It can be seen that increase in the magnetization of IR layer to the value $M_{sat} = 40$ kA/m leads to the frequency range expansion of SW signal by the value $\Delta f = 1$ GHz. Further, at $M_{sat} = 120$ kA/m the low-frequency boundary of the signal shifts by 300 MHz to the region of higher frequencies, which is accompanied by a sharpening of the output signal band. In this case, in the frequency region of 4.23 GHz a signal transmission region is formed when the level decreases by 30 db.

Next, we will consider the results of calculating the signal power spectral density in the region of each of the

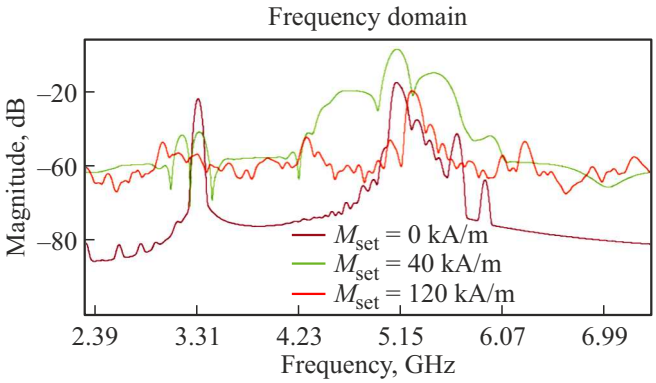

Figure 2. Amplitude-frequency curves for YIG microwaveguide with IR layer at its different magnetization.

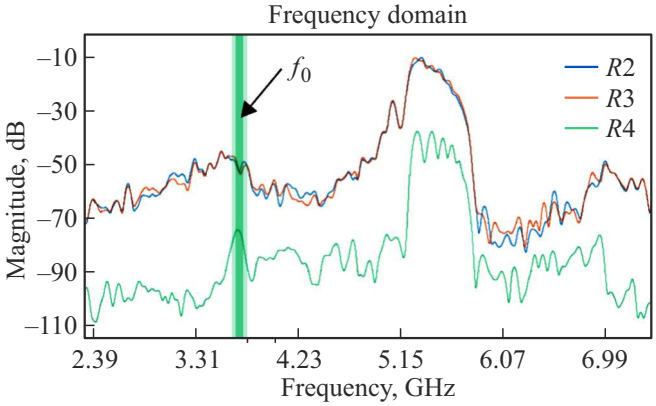

Figure 3. Amplitude-frequency curves for structure with iron-rhodium at its magnetization $M_{sat} = 120$ kA/m.

antennas R2, R3 and R4. Figure 3 shows AFC from various ports at IR magnetization of $M_{sat} = 120$ kA/m.

To study the influence of the magnetization value of IR layer on SW spectrum the numerical simulation of the propagation of the signal supplied to the input antenna at the frequency $f_0 = 3.38$ GHz was carried out. To identify the features that arise in the region of the output antennas, two-dimensional maps of the spatial distribution of SW intensity

$$I(x, y) = \sqrt{m_z^2(x, y) + m_x^2(x, y)}$$

in the microwaveguide were plotted at different values of the magnetization of IR layer.

Figure 4, *a* shows the intensity distribution map for the case when iron-rhodium is the antiferromagnet and $M_{sat} = 0$. When spin-wave signal is excited in the microwaveguide, the wide-width modes of the structure with transverse wave numbers $k_{y,n} = n\pi/w_1$ [25–27] are excited. When SW propagates, the interference of natural modes and wave attenuation are observed. With an increase in the temperature of the IR layer, which in experiments is usually achieved by laser irradiation or by Joule heating [16–20], with increase in the magnitude of IR magnetization to $M_{sat} = 40$ kA/m, the localization of SW intensity in region in YIG free of IR layer is observed. In this case, the signal intensity is concentrated at the interface of the two layers: IR and YIG (see Figure 4, *b*). A division of the SW intensity into three regions is observed: the first two coincide with YIG region not covered by the IR layer, and the third one is located under IR layer; In view of this we can make assumption about the occurrence of a distributed longitudinal coupling of SW through the region under IR layer, however, in the first two regions a significant concentration of SW intensity is observed. In this case, the system exhibits behavior similar to the spin-wave splitter or power coupler proposed in the paper [27]. Upon further increase in magnetization to $M_{sat} = 120$ kA/m, the concentration of SW intensity is observed in the third region, namely, the wave begins to propagate in a narrow channel inside YIG under IR layer, which is demonstrated in Figure 4, *c*.

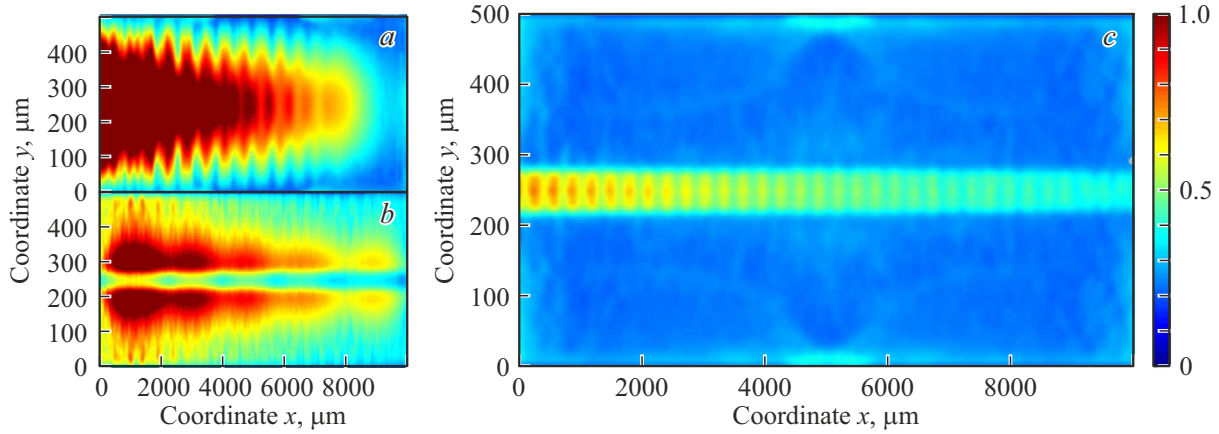

Figure 4. Maps of spatial distribution of spin wave intensity in structure with iron-rhodium at different magnetization values. *a* — magnetization distribution at $M_{sat} = 0$ kA/m; *b* — magnetization distribution at $M_{sat} = 40$ kA/m. (*c*) Magnetization distribution at $M_{sat} = 120$ kA/m.

4. Conclusion

As part of this study, a detailed analysis of frequency filtering modes was carried out based on the proposed method to control the propagation of spin waves in structure containing yttrium iron garnet (YIG) strip with IR strip. Analysis based on micromagnetic numerical simulation reveals the potential to control the properties of spin waves propagation in the composite structure. Based on the calculated amplitude-frequency curves of the spin-wave signal in the considered magnonic structure at different values of the magnetization of IR layer the modes of controlled spatial-frequency selection of spin waves are demonstrated. Thus, by changing the magnetization of the IR layer by point heating, it is possible to observe the spatial localization of the spin wave power in the regions of IR layer and regions of YIG film not covered by IR layer. In this case, localized propagation of the spin-wave beam is also observed in YIG region, precisely located under IR layer. The use of such structure makes it possible not only to control the spin waves propagation, but also to change the magnetoelectronics based on materials containing IR.

Funding

The paper was carried out with the financial support from the Russian Science Foundation, grant No. 23-29-00610.

Conflict of interest

The authors declare that they have no conflict of interest.

References

[1] V.E. Demidov, S. Urazhdin, G. de Loubens, O. Klein, V. Cros, A. Anane, S.O. Demokritov. Phys. Rep. **673**, 1 (2017).
[2] A. Khitun, M. Bao, K.L. Wang. J. Phys. D **43**, *26*, 264005 (2010).
[3] A.R. Safin, S.A. Nikitov, A.I. Kirilyuk, D.V. Kalyabin, A.V. Sadovnikov, P.A. Stremoukhov, M.V. Logunov, P.A. Popov. ZhETF **158**, 85 (2020). (in Russian).
[4] A.A. Amirov, V.V. Rodionov, I.A. Starkov, A.S. Starkov, A.M. Aliev. J. Magn. Magn. Mater. **470**, 77 (2019).
[5] Q. Wang, M. Kewenig, M. Schneider, R. Verba, F. Kohl, B. Heinz, M. Geilen, M. Mohseni, B. Lägel, F. Ciubotaru, C. Adelmann, C. Dubs, S.D. Cotofana, O.V. Dobrovolskiy, T. Bräher, P. Pirro, A.V. Chumak. Nature Electron. **3**, *12*, 765 (2020).
[6] S. Nikitin, G. Myalikgulyev, A. Tishin, M. Annaorazov, K. Asatryan, A. Tyurin. Phys. Lett. A **148**, 363 (1990).
[7] Y. Lee, Z.Q. Liu, J.T. Heron, J.D. Clarkson, J. Hong, C. Ko, M.D. Biegalski, U. Aschauer, S.L. Hsu, M.E. Nowakowski, J. Wu, H.M. Christen, S. Salahuddin, J.B. Bokor, N.A. Spaldin, D.G. Schlom, R. Ramesh. Nature Commun. **6**, 5959 (2015).
[8] A. Tohki, K. Aikoh, A. Iwase, K. Yoneda, S. Kosugi, K. Kume, T. Batchu-luun, R. Ishigami, T. Matsui. J. Appl. Phys. **111**, 07A742 (2012).
[9] A.I. Zakharov, A.M. Kadomtseva, R.Z. Levitin, E.G. Ponyatovskii. Sov. Phys. JETP **19**, 1348 (1964).
[10] M.P. Annaorazov, K.A. Asatryan, G. Myalikgulyev, S.A. Nikitin, A.M. Tishin, A.L. Tyurin. Cryogenics **32**, 867 (1992).
[11] J.S. Kouvel. J. Appl. Phys. **37**, 1257 (1966).
[12] R. Wayne. Phys. Rev. **170**, 523 (1968).
[13] A.A. Amirov, I.A. Baraban, A.A. Grachev, A.P. Kamantsev, V.V. Rodionov, D.M. Yusupov, V.V. Rodionova, A.V. Sadovnikov. AIP Adv. **10**, 025124 (2020).
[14] V.V. Kruglyak, S.O. Demokritov, D. Grundler. J. Phys. D **43**, 264001 (2010).
[15] Y.K. Fetisov, G. Srinivasan. Appl. Phys. Lett. **88**, *14*, 143503 (2006).
[16] Exceptional-point phase transition in coupled magnonic waveguides, A.V. Sadovnikov, A.A. Zyablovsky, A.V. Dorofeenko, S.A. Nikitov. Phys. Rev. Appl. **18**, 024073 (2022).
[17] A.P. Kamantsev, V.V. Koledov, A.V. Mashirov, E.T. Dilmieva, V.G. Shavrov, J. Cwik, I.S. Tereshina, M.V. Lyange, V.V. Khovaylo, G. Porcari, M. Topic. Bull. Russ. Acad. Sci. Phys. **79**, 1086 (2015).
[18] A. Sadovnikov, E. Beginin, S. Odincov, S. Sheshukova, Y. Sharaevskii, A.I. Stognij, S. Nikitov. Appl. Phys. Lett. **108**, 172411 (2016).
[19] A. Sadovnikov, A. Grachev, V. Gubanov, S. Odintsov, A. Martyshkin, S. Sheshukova, Y. Sharaevskii, S. Nikitov. Appl. Phys. Lett. **112**, 142402 (2018).
[20] S.A. Nikitov, A.R. Safin, D.V. Kalyabin, A.V. Sadovnikov, E.N. Beginin, M.V. Logunov, M.A. Morozova, S.A. Odintsov, S.A. Osokin, A.Yu. Sharaevskaya, Yu. P. Sharaevsky, A.I. Kirilyuk. UFN **190**, 1009 (2020). (in Russian).
[21] A. Barman, G. Gubbiotti, S. Ladak, A.O. Adeyeye, M. Krawczyk, J. Gräfe, C. Adelmann, S. Cotofana, A. Naeemi, V.I. Vasyuchka, B. Hillebrands, S.A. Nikitov, H. Yu, D. Grundler, A.V. Sadovnikov, A.A. Grachev, S.E. Sheshukova, J-Y. Duquesne, M. Marangolo, G. Csaba, W. Porod, V.E. Demidov, S. Urazhdin, S.O. Demokritov, E. Albisetti, D. Petti, R. Bertacco, H. Schultheiss, V.V. Kruglyak, V.D. Poimanov, S. Sahoo, J. Sinha, H. Yang, M. Münzenberg, T. Moriyama, S. Mizukami, P. Landeros, R.A. Gallardo, G. Carlotti, J-V. Kim, R.L. Stamps, R.E. Camley, B. Rana, Y. Otani, W. Yu, T. Yu, G.E.W. Bauer, C. Back, G.S. Uhrig, O.V. Dobrovolskiy, B. Budinska, H. Qin, S. van Dijken, A.V. Chumak, A. Khitun, D.E. Nikonov, I.A. Young, B.W. Zingsem, M. Winklhofer. J. Phys.: Condens. Matter **33**, 413001 (2021).
[22] D.D. Stancil, A. Prabhakar. Springer, N.Y. (2009).
[23] A.G. Gurevich, G.A. Melkov. Magnetization Oscillations and Waves. CRC Press, Boca Raton, FL, USA (1996).
[24] A. Vansteenkiste, J. Leliaert, M. Dvornik, M. Helsen, F. Garcia-Sanchez, B. Van Waeyenberge. AIP Adv. **4**, 107133 (2014).
[25] S.N. Bajpai. J. Appl. Phys. **58**, 910 (1985).
[26] T.W. O'Keeffe, R.W. Patterson. J. Appl. Phys. **49**, 4886 (1978).
[27] A.V. Sadovnikov, E.N. Beginin, S.E. Sheshukova, D.V. Romanenko, Yu.P. Sharaevskii, S.A. Nikitov. Appl. Phys. Lett. **107**, 202405 (2015).

Translated by I.Mazurov